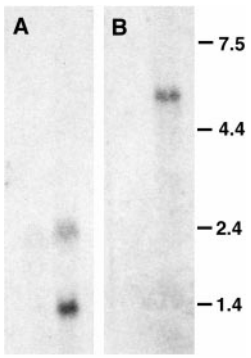

Fig. 4. Retrotransposon expression in *cmt3* mutants. Blots containing 40 μg of total RNA from whole shoots of line *clk-st* (left) or *cmt3-7* (right) were hybridized with either an Athila probe (**A**) or a Ta3 probe (**B**) (*10*). The positions of molecular size markers (in kilobases) are indicated.

instance, *SUP* and the Ta3 retrotransposon appear to depend more heavily on CpXpG methylation, whereas FWA and possibly Tar17 rely more on CpG methylation. Athila sequences require both types of methylation, because Athila-related transcripts are activated in both *cmt3* and *met1* mutants.

Despite a nearly complete loss of genomic CpXpG methylation, null *cmt3* mutants are morphologically normal, even after five generations of inbreeding. In contrast, *met1* mutants exhibit severe developmental abnormalities (*3, 7*). One explanation for this is that CpXpG and CpG methylation may act in a partially redundant fashion to silence most genes. Viability despite severe loss of genomic methylation makes *Arabidopsis* an ideal model system for elucidating the roles of DNA methylation in epigenetic and developmental processes.

References and Notes

1. T. Bestor, A. Laudano, R. Mattaliano, V. Ingram, *J. Mol. Biol.* **203**, 971 (1988).
2. M. J. Ronemus, M. Galbiati, C. Ticknor, J. Chen, S. L. Dellaporta, *Science* **273**, 654 (1996).
3. E. J. Finnegan, W. J. Peacock, E. S. Dennis, *Proc. Natl. Acad. Sci. U.S.A.* **93**, 8449 (1996).
4. Y. Gruenbaum, T. Naveh-Many, H. Cedar, A. Razin, *Nature* **292**, 860 (1981).
5. A. Vongs, T. Kakutani, R. A. Martienssen, E. J. Richards, *Science* **260**, 1926 (1993).
6. S. E. Jacobsen, E. M. Meyerowitz, *Science* **277**, 1100 (1997).
7. S. E. Jacobsen, H. Sakai, E. J. Finnegan, X. Cao, E. M. Meyerowitz, *Curr. Biol.* **10**, 179 (2000).
8. N. Kishimoto *et al.*, *Plant Mol. Biol.*, in press.
9. S. B. Baylin, J. G. Herman, *Trends Genet.* **16**, 168 (2000).
10. For supplemental data and methods, see *Science* Online (www.sciencemag.org/cgi/content/full/1059745/DC1).
11. S. Henikoff, L. Comai, *Genetics* **149**, 307 (1998).
12. I. Callebaut, J. C. Courvalin, J. P. Mornon, *FEBS Lett.* **446**, 189 (1999).
13. C. M. McCallum, L. Comai, E. A. Greene, S. Henikoff, *Nature Biotechnol.* **18**, 455 (2000).
14. X. Cheng, *Annu. Rev. Biophys. Biomol. Struct.* **24**, 293 (1995).
15. T. Pelissier, S. Tutois, S. Tourmente, J. M. Deragon, G. Picard, *Genetica* **97**, 141 (1996).
16. W. J. Soppe *et al.*, *Mol. Cell* **6**, 791 (2000).
17. A. Konieczny, D. F. Voytas, M. P. Cummings, F. M. Ausubel, *Genetics* **127**, 801 (1991).
18. A. Steimer *et al.*, *Plant Cell* **12**, 1165 (2000).
19. H. Hirochika, H. Okamoto, T. Kakutani, *Plant Cell* **12**, 357 (2000).
20. S. Pradhan, R. L. Adams, *Plant J.* **7**, 471 (1995).
21. C. M. Papa, N. M. Springer, M. G. Muszynski, S. M. Kaeppler, unpublished data.
22. E. J. Finnegan, K. A. Kovac, *Plant Mol. Biol.* **43**, 189 (2000).
23. T. M. Rose *et al.*, *Nucleic Acids Res.* **26**, 1628 (1998).

24. Supported by NIH grant GM60398, a Beckman Young Investigator grant, a Searle Scholar award (S.E.J.), NIH training grants GM07104 (J.P.J.) and GM07185 (D.Z.), and NIH grant GM29009 (S.H.). We thank C. Hyun, M. Huang, L. Cahoon, and H. Le for technical assistance; S. Kaeppler and N. Springer for helpful discussions; and E. Richards for the *met1* mutant.

9 February 2001; accepted 23 April 2001
Published online 10 May 2001;
10.1126/science.1059745
Include this information when citing this paper.

Ordering Genes in a Flagella Pathway by Analysis of Expression Kinetics from Living Bacteria

S. Kalir,[1] J. McClure,[3] K. Pabbaraju,[3] C. Southward,[3] M. Ronen,[1] S. Leibler,[4] M. G. Surette,[3] U. Alon[1,2]*

The recent advances in large-scale monitoring of gene expression raise the challenge of mapping systems on the basis of kinetic expression data in living cells. To address this, we measured promoter activity in the flagellar system of *Escherichia coli* at high accuracy and temporal resolution by means of reporter plasmids. The genes in the pathway were ordered by analysis algorithms without dependence on mutant strains. The observed temporal program of transcription was much more detailed than was previously thought and was associated with multiple steps of flagella assembly.

Under the proper conditions, the bacterium *E. coli* synthesizes multiple flagella, which allow it to swim rapidly. Classical genetics showed that the 14 flagella operons are arranged in a regulatory cascade of three classes (*1*–*5*) (Fig. 1). The class 1 operon encodes the transcriptional activator of class 2 operons. Class 2 genes include structural components of a rotary motor called the basal body–hook structure, as well as the transcriptional activator for class 3 operons. Class 3 includes flagellar filament structural genes and the chemotaxis signal transduction system that directs the cells' motion. A checkpoint mechanism ensures that class 3 genes are not transcribed before functional basal body–hook structures are completed (Fig. 1).

Here, we developed a system for real-time monitoring of the transcriptional activation of the flagellar operons by means of a panel of 14 reporter plasmids in which green fluorescent protein (GFP) (*6*) is under the control of one of the flagellar promoters (*7*). This allowed us to extend previous timing studies that depended on lacZ fusions to up to four operons (*8*, *9*). Use of GFP eliminates the need for cell lysis required for lacZ and DNA microarray studies (*10*–*13*). Therefore, the present system makes it possible to measure accurately continuous time courses from living cells grown in a multiwell

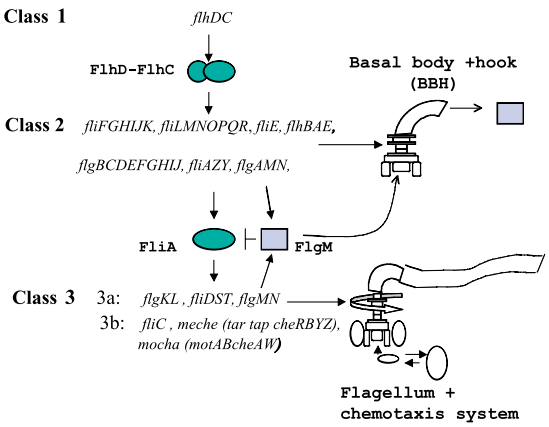

Fig. 1. The genetically defined hierarchy of flagellar operons in *Escherichia coli* (*1, 2*). The master regulator FlhDC turns on class 2 genes, one of which, FliA, turns on class 3 genes. A checkpoint ensures that class 3 genes are not turned on until basal body–hook structures (BBH) are completed. This is implemented by FlgM, which binds and inhibits FliA. When BBH are completed, they export FlgM out of the cell, leaving FliA free to activate the class 3 operons (*9*, *27*, *28*). Note that *flgM* is transcribed from both a class 2 (*flgAMN*) and a class 3 (*flgMN*) promoter.

plate fluorimeter (*14*). Average errors between repeat experiments were less than 10%, compared with errors of at least twofold often associated with expression assays requiring cell lysis and manipulation (*10*–*12*).

The flagella system is turned on during the exponential phase of growth. Clustering the fluorescence levels of the operons (Fig. 2A) according to similarity in their expression profiles (*10*–*13*) showed that they fall into clusters that correspond to the genetically defined classes 1 and 2 (Fig. 2B). Three of the six class 3 operons are close to the compact class 2 cluster, and the other three are in a separate cluster. This separation is based mainly on different coordinated responses of the operon classes. To determine the timing order, we extended the clustering algorithm with a temporal labeling procedure that hierarchically orders the clusters according to the relative timing of their average expression profiles. Log fluorescence of each reporter strain, normalized by its maximum for each experiment, was set to zero mean and variance one, and clustered by means of a standard single-linkage algorithm with a Euclidean metric (Matlab 5.3, Mathworks) (*15*). In general, clustering algorithms do not specify an ordering of the clusters. In the resulting dendrograms, as the data are split hierarchically into a tree, pairs of subtrees in each splitting are placed in an arbitrary order. To define the temporal order of expression, we first considered each splitting from the top down and computed the average log fluorescence (normalized by the maximal fluorescence) for the two subtrees, $\log(f_1)$ and $\log(f_2)$. Next, we computed $t_i = -\int \log[f_i(t)]dt$ (generally the earlier a sigmoidal curve rises, the smaller its t_i. Since log fluorescence is used, the initial rise timing is emphasized.) The subtree with the smaller t_i was then positioned to the left. The present algorithm was able to correctly order simulated gene cascades. The algorithm is available upon request or at www.weizmann.ac.il/mcb/UriAlon.

The algorithm arranged the operons in the order: class 1 followed by class 2 followed by class 3 (*8*, *9*) (Fig. 2B). Within the class 2 cluster, the promoters were turned on sequentially, with significant delays, in the order *fliL*, *fliE*, *fliF*, *flgA*, *flgB*, *flhB*, and *fliA* (Fig. 2). The observed order corresponds to the spatial position of the gene products during flagellar motor assembly, going from the cytoplasmic to the extracellular sides (*1*, *2*) (Fig. 3). The *fliL* operon genes form the cytoplasmic C ring, and *fliE* and *fliF* genes form the MS ring in the inner membrane, thought to be the first assembled structure (*1*). The *flgA*, *flhB*, and *flgB* genes participate in the export and formation of the periplasmic rod, the distal rings in the outer membrane, and the extracellular hook. The transcription factor responsible for turning on class 3

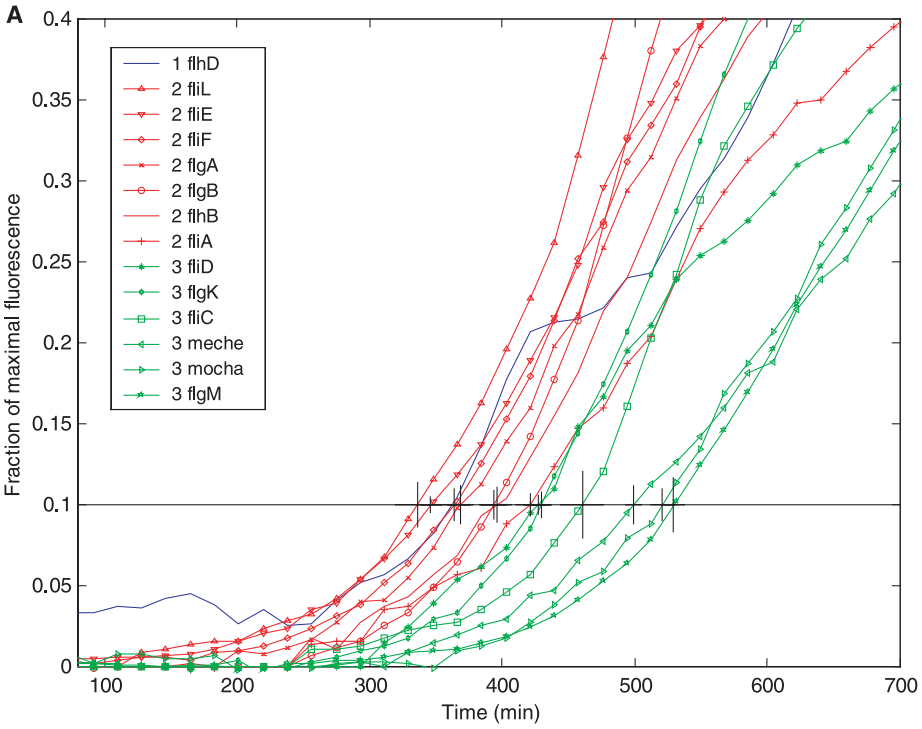

Fig. 2. (**A**) Fluorescence of flagella reporter strains as a function of time, normalized by the maximal fluorescence of each strain. Average of five experiments in growth condition A (see below) are shown (bars, SD). Class 1, 2, and 3 operons are marked in blue, red, and green, respectively. (**B**) Fluorescence of flagella reporter strains as a function of time for two experimental conditions. Log intensity of each promoter, normalized by its maximal value in each experiment, scales from blue (low) to red (high). Operons are arranged according to the temporal clustering results. The first 630 minutes of each experiment, for two growth conditions, with and without preexisting flagella, are shown. Condition A: Stationary-phase cultures with two to five flagella per cell (*29*) are diluted 1:600 into fresh medium; induction of new flagella begins after about three to four generations, and thus old flagella are diluted out by cell division to a degree that most cells have no preexisting flagella. Condition B: Overnight cultures are diluted 1:60. The flagellar operons are turned on within one cell generation so that old flagella are present. The presence or absence of preexisting flagella was verified by microscopic observation of cell motility as described (*23*). Dendrogram shows hierarchical gene clustering and temporal order. The statistical significance (*P* value) for temporal ordering at each splitting was determined by the fraction of times that a larger $|t_1 - t_2|$ value was found upon clustering and labeling 1000 randomized data sets generated by randomly permuting the gene coordinates at each time point. Similarly, a *P* value for clusters was determined by the fraction of times that a larger splitting distance occurred in the randomized data sets. Clusters with significance $P < 0.001$ are marked with filled triangles; $P \approx 0.01$ with an open triangle; and $P > 0.01$, no triangles. Temporal ordering of all tree splittings is significant ($P < 0.01$), except the splittings marked with a star.

[1]Department of Molecular Cell Biology, [2]Department of Physics of Complex Systems, Weizmann Institute of Science, Rehovot 76100, Israel. [3]Department of Microbiology and Infectious Diseases, University of Calgary, Calgary, AB, Canada T2N 4N1. [4]Howard Hughes Medical Institute, Departments of Molecular Biology and Physics, Princeton University, Princeton, NJ 08544, USA.

*To whom correspondence should be addressed. E-mail: urialon@weizmann.ac.il

genes, *fliA*, is the last class 2 gene to turn on.

A separation of class 3 genes into two kinetic groups was seen, with the filament structural operons *flgK*, *fliD*, and *fliC* activated first, and *flgM* and the chemotaxis operons *meche* and *mocha* going on only after a substantial delay (Fig. 2). Thus, the hardware for the flagellar propeller is expressed before the chemotaxis navigation system (Fig. 3). The genes for motor torque generation, *motAB* in the *mocha* operon, are in the late class 3 group, and indeed, it has been shown that they can be functionally incorporated long after motors are assembled (*16*, *17*).

When flagella were induced in cells with no preexisting flagella, a temporal separation between most class 2 genes and class 3 genes was observed (Fig. 2B, condition A); whereas in cells with preexisting flagella, the delay between class 2 and the early class 3 genes decreased drastically (Fig. 2B, condition B). This probably reflects the checkpoint in flagella biosynthesis (Fig. 1). When preexisting flagella are present, newly synthesized FlgM is exported from the cells even before new basal bodies are completed. This frees FliA to turn on class 3 genes at an earlier time. Such memory effects may be a general kinetic signature of regulatory checkpoints.

A simple hypothesis for the mechanism underlying the temporal order of promoter activation within classes 2 and 3 is that the DNA regulatory sites in the promoter regions of the operons are ranked in affinity. As the concentration of the relevant transcription factor (FlhDC, FliA) gradually increases in the cell, it first binds and activates the operons with the highest affinity sites, and only later does it bind and activate operons with lower affinity sites.

The standard genetic method of pathway analysis suffers from the limitation that conclusions drawn from mutant cells sometimes apply to a physiological state far from wild-type. The present kinetic analysis can complement genetics by probing cells with an intact regulatory system, rather than mutant cells. For example, class 3 operons were subdivided by mutant analysis into class "3a" and class "3b" (Fig. 1), based on residual expression in a *fliA* mutant of class 3a but not 3b operons (*1*). This mutant may exemplify a situation never reached by wild-type cells (high FlhDC but no FliA). The present kinetic subdivision of class 3 operons into early and late temporal groups hints at a functionally reasonable order.

The precise order of transcription of the various operons is probably not essential for assembling functional flagella. This is suggested by complementation experiments in which the motility of flagella mutants was rescued by expression of the wild-type gene from a foreign promoter (*1*). The detailed transcription order could, however, function to make flagella synthesis more efficient, because parts are not transcribed earlier than needed. From the viewpoint of reverse engineering, this may be exploited to decipher detailed assembly steps from transcription data.

The present experimental method can be readily applied to gene systems in a broad range of sequenced prokaryotes, as well as to eukaryotic genes with well-defined regulatory regions. For example, GFP was used to monitor gene expression on a large scale in yeast (*18*). Studies on various systems could establish whether temporal clustering and memory effects can be a general method in mapping assembly cascades and detecting regulatory checkpoints. It would be important to discover whether, in analogy to the systems-identification principals of engineering, there are ways of mapping additional system motifs, such as feedback loops, by using detailed expression measurements.

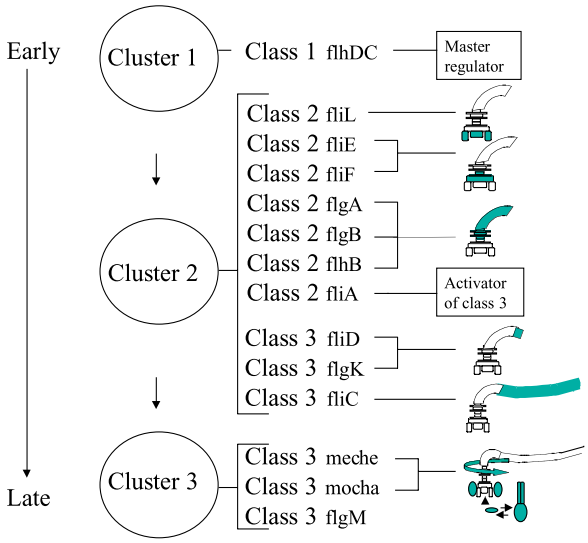

Fig. 3. Present kinetic classification of the flagellar operons. The three clusters and the operons within each cluster are arranged by their relative timing according to the temporal clustering results. Positions of the corresponding gene products in the flagellum (*1*) are indicated in green.

References and Notes

1. R. Macnab, in Escherichia coli *and* Salmonella: *Cellular and Molecular Biology*, F. C. Neidhart, Ed. (American Society for Microbiology, Washington DC, 1996), pp. 123–145.
2. G. S. Chilcott, K. T. Hughes, *Microbiol. Mol. Biol. Rev.* **64**, 694. (2000).
3. K. Kutsukake, Y. Ohya, T. Iino, *J. Bacteriol.* **172**, 741 (1990).
4. Y. Komeda, *J. Bacteriol.* **168**, 1315 (1986).
5. Y. Komeda, *J. Bacteriol.* **150**, 16 (1982).
6. B. P. Cormack, R. H. Valdivia, S. Falkow, *Gene* **173**, 33 (1996).
7. RP437 (*19*) and YK410 (*20*) are *E. coli* K12 strains that are wild type for motility and chemotaxis. The polymerase chain reaction was used to amplify the flagellar promoter regions using primers designed from the MG1655 genome sequence (*21*). The promoter region coordinates are flhD (1976454–1976212), flgB (1130044–1130245), flgA (1130245–1130044), fliA (2000123–1999779), fliD (2001594–2001916), fliC (2001916–2001594), fliE (2011261–2010998), fliF (2010998–2011261), fliL (2017491–2017644), meche (1970893–1970676), mocha (1975301–1975161), flgM (1129471–1129331), flgK (1137467–1137656), and flhB (1964392–1964190). Reporter plasmids were constructed by subcloning these promoter regions into a Bam HI site upstream of a promoterless GFP on the low-copy vector pCS21. pCS21 was constructed by replacing the luciferase gene of pZS21-luc (*22*) with a DNA fragment containing the *GFPmut3* (*6*) gene. Promoter identity was verified by sequencing. There was no observable effect of the plasmids on swimming motility as assayed on soft agar plates [performed as described (*23*)], suggesting that the system can compensate for the extra promoter copies introduced by these low-copy plasmids. There were no measurable differences in the growth rate of the reporter strains, with the exception of the reporters for *meche*, *mocha*, and *flgM*, which show a somewhat faster growth in culture. The effective delay in activation of these late class 3 reporters would be further enhanced if one takes into account their faster growth.
8. B. M. Pruss, P. Matsumura, *J. Bacteriol.* **179**, 5602 (1997).
9. J. E. Karlinsey *et al.*, *Mol. Microbiol.* **37**, 1220 (2000).
10. P. T. Spellman *et al.*, *Mol. Biol. Cell* **9**, 3273 (1998).
11. R. Zhao *et al.*, *Genes Dev.* **14**, 981 (2000).
12. S. Chu *et al.*, *Science* **282**, 699 (1998).
13. M. B. Eisen, P. T. Spellman, P. O. Brown, D. Botstein, *Proc. Natl. Acad. Sci. U.S.A.* **95**, 14863 (1998).
14. Cultures (2 ml) inoculated from single colonies were grown 16 hours in Tryptone broth (Bio 101, Inc.) with kanamycin (25 μg/ml) at 37°C with shaking at 300 rpm. The cultures were diluted 1:600 or 1:60 into defined medium [M9 minimal salts (Bio 101, Inc.) + 0.1 mM $CaCl_2$ + 2 mM $MgSO_4$ + 0.4% glycerol + 0.1% casamino acids + kanamycin], at a final volume of 150 μl per well in flat-bottomed 96-well plates (Sarsteadt 82.1581.001). The cultures were covered by a 100-μl layer of mineral oil (Sigma M-3516) to prevent evaporation during measurement. Cultures were grown in a Wallac Victor2 multiwell fluorimeter set at 30°C and assayed with an automatically repeating protocol of shaking (1 mm orbital, normal speed, 180 s), fluorescence readings (filters F485, F535, 0.5 s, CW lamp energy 10,000), and absorbance (OD) measurements (600 nm, P600 filter, 0.1 s). Time between repeated measurements was 6 min. Background fluorescence of cells bearing a promotorless GFP vector was subtracted. RP437 was the parental strain of all reporter strains, except *flhDC*, for which the signal was below background at early time points, and thus YK410 was used. Similar timing and temporal ordering of the flagellar operons was observed in this strain. The high temporal resolution of the present system benefits from the apparent rapid activation of GFP in bacteria (*24*, *25*) as compared with reported times for folding and oxidation of the chromophore in vitro, 10 min and 1 hour, respectively (*26*). The detailed timing of expression observed in the experiments described here implies that the onset of flagella biosynthesis may be synchronized within the population. This may involve metabolic

effects as the bacteria are shifted from stationary phase in a rich medium to growth in a more minimal medium. The mechanism for synchronization is not understood but may involve secreted factors, such as signaling molecules, that are diluted out and need to be generated over time. We are currently investigating this phenomenon.
15. R. O. Duda, P. E. Hart, *Pattern Classification and Scene Analysis* (Wiley, New York, 1973).
16. D. F. Blair, H. C. Berg, *Science* **242**, 1678 (1988).
17. S. M. Block, H. C. Berg, *Nature* **309**, 470 (1984).
18. D. Dimster-Denk *et al.*, *J. Lipid Res.* **40**, 850 (1999).
19. J. S. Parkinson, S. E. Houts, *J. Bacteriol.* **151**, 106 (1982).
20. Y. Komeda, K. Kutsukake, T. Iino, *Genetics* **94**, 277 (1980).
21. F. R. Blattner *et al.*, *Science* **277**, 1453 (1997).
22. R. Lutz, H. Bujard, *Nucleic Acids Res.* **25**, 1203 (1997).
23. U. Alon, M. G. Surette, N. Barkai, S. Leibler, *Nature* **397**, 168 (1999).
24. P. Cluzel, M. Surette, S. Leibler, *Science* **287**, 1652 (2000).
25. G. S. Waldo, B. M. Standish, J. Berendzen, T. C. Terwilliger, *Nature Biotechnol.* **17**, 691 (1999).
26. B. G. Reid, G. C. Flynn, *Biochemistry* **36**, 6786 (1997).
27. K. Ohnishi, K. Kutsukake, H. Suzuki, T. Iino, *Mol. Microbiol.* **6**, 3149 (1992).
28. K. T. Hughes, K. L. Gillen, M. J. Semon, J. E. Karlinsey, *Science* **262**, 1277 (1993).
29. C. D. Amsler, M. Cho, P. Matsumura, *J. Bacteriol.* **175**, 6238 (1993).
30. We thank M. Elowitz, R. Kishony, C. Guet, W. Hsing, M. Eisenbach, P. Bashkin, N. Rosenfeld, R. Rosenberg, S. Shen-Or, E. Levine, G. Ziv, A. Sigal, N. Barkai, E. Siggia, and T. Silhavy for discussions. We also thank J. Parkinson and R. Macnab for strains. This work was supported by the Human Frontiers Science Project, Canadian Institute of Health Research (M.S.), the Alberta Heritage Foundation for Medical Research (M.S.), the Israel Science Foundation (U.A.), the Charpak-Vered Fellowship (U.A.), and the U.S. National Institutes of Health (S.L.).

3 January 2001; accepted 11 May 2001

Vitamin C–Induced Decomposition of Lipid Hydroperoxides to Endogenous Genotoxins

Seon Hwa Lee, Tomoyuki Oe, Ian A. Blair*

Epidemiological data suggest that dietary antioxidants play a protective role against cancer. This has led to the proposal that dietary supplementation with antioxidants such as vitamin C (vit C) may be useful in disease prevention. However, vit C has proved to be ineffective in cancer chemoprevention studies. In addition, concerns have been raised over potentially deleterious transition metal ion–mediated pro-oxidant effects. We have now determined that vit C induces lipid hydroperoxide decomposition to the DNA-reactive bifunctional electrophiles 4-oxo-2-nonenal, 4,5-epoxy-2(*E*)-decenal, and 4-hydroxy-2-nonenal. The compound 4,5-Epoxy-2(*E*)-decenal is a precursor of etheno-2′-deoxyadenosine, a highly mutagenic lesion found in human DNA. Vitamin C–mediated formation of genotoxins from lipid hydroperoxides in the absence of transition metal ions could help explain its lack of efficacy as a cancer chemoprevention agent.

Molecular oxygen undergoes three successive one-electron reductions (*1*) to reactive oxygen species (ROS) that can damage cellular macromolecules such as DNA and proteins (*2*). DNA damage results directly from ROS (*3*) or from ROS-derived lipid hydroperoxides that break down to form endogenous genotoxins (*4*, *5*). Covalent modifications to DNA by ROS (*6*) and lipid hydroperoxide–derived genotoxins (*7*, *8*) have been unequivocally characterized in mammalian DNA. Lipid hydroperoxides are formed nonenzymatically by the action of ROS on polyunsaturated fatty acids (PUFAs) (*4*) or enzymatically from lipoxygenases (LOXs) (*9*) and cyclooxygenases (COXs) (*10*). Linoleic acid, the major ω-6 PUFA present in plasma lipids, is converted to 13(*S*)-hydroperoxy-(*Z,E*)-9,11-octadecadienoic acid (13-HPODE) by human 15-LOX (*11*). COX-1 and COX-2 produce mainly 9(*R*)-hydroperoxy-(*E,Z*)-10,12-octadecadienoic acid (9-HPODE) and 13-HPODE (*10*). The HPODEs are subsequently reduced to the corresponding 9(*R*)- and 13(*S*)-hydroxy-octadecadienoic acids (HODEs) through the peroxidase activity of the COXs (*12*, *13*).

Lipid hydroperoxides undergo transition metal ion–dependent decomposition to the α,β-unsaturated aldehyde genotoxins 4-oxo-2-nonenal and 4-hydroxy-2-nonenal (*14*). 4-Oxo-2-nonenal is a particularly potent lipid hydroperoxide–derived genotoxin (*15*), which reacts with DNA bases to form heptanone-etheno-adducts (Fig. 1) (*16*). Failure to repair these DNA lesions can lead to mutations (*4, 5*) or apoptosis (*17*). The use of vitamin C (vit C) for antioxidant therapy has been advocated because of its ability to scavenge ROS, although its potential for prooxidant activity in the presence of transition metal ions has also been recognized (*18*). Transition metal ion–mediated decomposition of lipid hydroperoxides is thought to be initiated by a one-electron reduction to an alkoxy radical (*14*, *19*). This raised the possibility that an alkoxy radical intermediate would also be formed by a one-electron reduction of the lipid hydroperoxide by vit C (Fig. 1). When a one-electron reduction of hydrogen peroxide occurs, the resulting hydroxy radical (*1*) is scavenged through a termination reaction either with the vit C radical anion (*20*) or with vit C itself. We reasoned that when an alkoxy radical is attached to a PUFA, intramolecular radical propagation could proceed more rapidly than intermolecular vit C–mediated termination reactions. Therefore, the same α,β-unsaturated aldehyde genotoxins observed with transition metal ions (*14*) may also be observed during vit C–induced decomposition of lipid hydroperoxides (Fig. 1). We have developed liquid chromatography (LC)/atmospheric pressure chemical ionization (APCI)/mass spectrometry (MS)/ultraviolet (UV) methodology to identify the α,β-unsaturated aldehydic bifunctional electrophiles 4,5-epoxy-2(*E*)-decenal (*21*), 4-oxo-2-nonenal (*14*), 4-hydroperoxy-2-nonenal (*14*, *22*), and 4-hydroxy-2-nonenal (*14*) that could potentially be formed during homolytic lipid hydroperoxide decomposition (Fig. 2) (*23–25*).

The prototypic ω-6 lipid hydroperoxide 13-HPODE was allowed to decompose in the presence of vit C in Chelex-treated Mops buffer at pH 7.0 and 37°C. Reaction products were then analyzed by LC/APCI/MS with concomitant UV monitoring (*24*). At early time points, 4-hydroperoxy-2-nonenal was the major product. After 30 min, the 4-hydroperoxy-2-nonenal level started to decline slowly with a concomitant increase in *trans*-4,5-epoxy-2(*E*)-decenal, 4-oxo-2-nonenal, and 4-hydroxy-2-nonenal. The reaction was complete at 2 hours, with 4-oxo-2-nonenal, 4-hydroperoxy-2-nonenal, and 4-hydroxy-2-nonenal as the major products (Fig. 3A). At higher vit C concentrations, *trans*-4,5-epoxy-2(*E*)-decenal, 4-oxo-2-nonenal, and 4-hydroxy-2-nonenal were produced in greater amounts, and *cis*-4,5-epoxy-2(*E*)-decenal could be readily detected (Fig. 3B). The level of 4-hydroperoxy-2-nonenal declined much more rapidly, so that after 2 hours it was undetectable. Unequivocal proof of structure for the aldehydes was obtained by normal-phase LC/tandem MS (MS/MS) analysis (*23*, *24*).

In separate experiments, 13-HPODE was

Center for Cancer Pharmacology, University of Pennsylvania, 1254 BRB II/III, 421 Curie Boulevard, Philadelphia, PA 19104–6160, USA.

*To whom correspondence should be addressed. E-mail: ian@spirit.gcrc.upenn.edu